Alteration of P-Type Calcium Channel Gating by the Spider Toxin ω-Aga-IVA

Stefan I. McDonough, Isabelle M. Mintz, and Bruce P. Bean
Department of Neurobiology, Harvard Medical School, Boston, Massachusetts 02115, and Vollum Institute, Oregon Health Sciences University, Portland, Oregon 97201 USA

ABSTRACT We studied the mechanism of inhibition of P-type calcium channels in rat cerebellar Purkinje neurons by the peptide toxin ω-Aga-IVA. Saturating concentrations of ω-Aga-IVA (>50 nM) inhibited inward current carried by 2–5 mM Ba almost completely. However, outward current at depolarizations of >+60 mV, carried by internal Cs, was inhibited much less, as was the tail current after such depolarizations. ω-Aga-IVA shifted the midpoint of the tail current activation curve by about +50 mV and made the curve less steep. The inactivation curve was also shifted in the depolarized direction and was made less steep. With ω-Aga-IVA, channels activated more slowly and deactivated more quickly than in control. Trains of repeated large depolarizations relieved the inhibition of current (as tested with moderate depolarizations), probably reflecting the unbinding of toxin. The relief of inhibition was faster with increasing depolarization, but did not require internal permeant ions. We conclude that ω-Aga-IVA alters voltage-dependent gating by stabilizing closed states of the channel and that ω-Aga-IVA dissociates much more rapidly from open channels than from closed.

INTRODUCTION

ω-Aga-IVA, a 48-amino acid peptide from the venom of the funnel web spider *Agelenopsis aperta* (Adams et al., 1993), inhibits over 90% of the high-voltage-activated calcium current in cerebellar Purkinje neurons (Mintz et al., 1992a,b). Channels sensitive to ω-Aga-IVA are found in many mammalian neurons, and the toxin has a high degree of selectivity, with no effect on L-type or N-type calcium channels (Eliot and Johnston, 1994; Mintz et al., 1992a; Randall and Tsien, 1995; Magnelli et al., 1995; Wu and Saggau, 1994; Bargas et al., 1994). Sensitivity to ω-Aga-IVA was initially used to define "P-type" calcium channels (Mintz et al., 1992a), using the name given earlier to the predominant current in Purkinje neurons (Llinás et al., 1989). Subsequently it has been proposed that the toxin also inhibits, with lower potency, a distinct "Q-type" channel (Randall and Tsien, 1995; see also McDonough et al., 1996; Tottene et al., 1996). Channels sensitive to ω-Aga-IVA contribute a major part of the calcium entry underlying synaptic transmission at a variety of central synapses (Turner et al., 1992; Wheeler et al., 1994; Regehr and Mintz, 1994).

Here we have studied the mechanism by which ω-Aga-IVA inhibits P-type calcium channels in cerebellar Purkinje neurons. We find that the toxin does not block the channel pore, but rather alters the voltage-dependent gating of the channels, so that they cannot be opened by moderate depolarizations. With strong depolarizations, channels can open with the toxin still bound. The instantaneous current-voltage relationship for open, toxin-bound channels was indistinguishable from control. Channel deactivation was faster with ω-Aga-IVA. Both with and without toxin, the deactivation time constant varied with duration of the activating pulse, suggesting a second open state. With repeated strong depolarizations, toxin unbinds from the channel. The relief of block can be understood if strong depolarizations cause a change in the channel conformation that alters the external toxin binding site allosterically.

MATERIALS AND METHODS

Cell preparation

Purkinje neurons were isolated from the brains of 6–21-day-old Long-Evans rats with slight modification of procedures described previously (Mintz et al., 1992a; McDonough et al., 1996). Briefly, cerebellar chunks were removed into ice-cold dissociation solution, consisting of 82 mM Na_2SO_4, 30 mM K_2SO_4, 5 mM $MgCl_2$, 10 mM HEPES, 10 mM glucose, and 0.001% phenol red indicator (pH 7.4, adjusted with NaOH). Cerebellar vermis was cut into ~1-mm^3 pieces, which were transferred into the dissociation solution with 3 mg/ml protease XXIII (Sigma, St Louis, MO) and incubated at 37°C for 7–8 min. The tissue was transferred to dissociation solution with added 1 mg/ml trypsin inhibitor (Sigma) and 1 mg/ml bovine serum albumin (Sigma) (pH 7.4, adjusted with NaOH) and cooled to room temperature under oxygen. Dissociation solution was then replaced by Tyrode's solution (150 mM NaCl, 4 mM KCl, 2 mM $CaCl_2$, 2 mM $MgCl_2$, 10 mM glucose, 10 mM HEPES, pH 7.4 with NaOH), and cells were stored at room temperature under oxygen for up to 6 h. Purkinje cells were isolated by gentle trituration in Tyrode's solution (~20 passages through the tip of a fire-polished Pasteur pipette) and allowed to settle to the bottom of the recording chamber. Purkinje neurons were identified morphologically by their large cell bodies (15–25 μm diameter) with a single dendritic stump.

Received for publication 23 September 1996 and in final form 28 January 1997.

Address reprint requests to Dr. Stefan I. McDonough, Department of Neurobiology, Harvard Medical School, 220 Longwood Ave., Boston, MA 02115. Tel.: 617-432-1768; Fax: 617-432-3057.

Dr. Mintz's present address is Department of Pharmacology and Experimental Therapeutics, Boston University School of Medicine, 80 East Concord Street, Boston, MA 02118.

0006-3495/97/05/2117/12 $2.00

Electrophysiological methods

Barium currents through voltage-activated calcium channels were recorded using the whole-cell configuration of the patch-clamp technique (Hamill et al., 1981). Patch pipettes were made from borosilicate glass tubing (Borralex; Dynalab, Rochester, NY) coated with Sylgard (Dow Corning Corp., Midland, MI) and fire-polished. Pipettes had resistances of 0.5–3 MΩ when filled with internal solution. After establishment of the whole-cell recording configuration, the cell was lifted off the bottom of the dish and positioned in front of an array of 12 perfusion tubes made of 250-μm internal diameter quartz tubing connected by Teflon tubing to glass reservoirs.

Currents were recorded with an Axopatch 200A amplifier (Axon Instruments, Foster City, CA), filtered with a corner frequency of 5 kHz (4-pole Bessel filter), digitized (10–50 kHz) using a Digidata 1200 interface and pClamp6 software (Axon Instruments), and stored on a computer. Some experiments were done using a List EPC-7 amplifier with Acquire software using a FASTLAB interface (Indec Systems, Sunnyvale, CA). Compensation (typically 80–95%) for series resistance (typically ~2.5 times higher than the pipette resistance) was employed. Only data from cells with uncompensated series resistance and current small enough to give a voltage error of less than 5 mV were analyzed. Calcium channel currents were corrected for leak and capacitive currents, either by applying 300 μM $CdCl_2$ to block Ca channel current or by subtracting a scaled current elicited by a 10-mV hyperpolarization from −80 mV. For recording of nonlinear charge movements, leak subtraction was done by subtracting a scaled current from voltage jumps between −110 mV and −130 mV, or between −120 mV and −140 mV.

Solutions

The standard internal solution was 56 mM CsCl, 68 mM CsF, 2.2 mM $MgCl_2$, 4.5 mM EGTA, 9 mM HEPES, 4 mM MgATP, 14 mM creatine phosphate (Tris salt), 0.3 mM GTP (Tris salt), pH 7.4, adjusted with CsOH. The standard external solution contained 2 mM $BaCl_2$, 160 mM tetraethylammonium (TEA) Cl, 10 mM HEPES, pH 7.4 with TEAOH, with 0.6 μM tetrodotoxin to block outward Cs currents through Na channels, 5 μM nimodipine to block L-type calcium channels, 1 μM ω-conotoxin GVIA to block N-type calcium channels, and 1 mg/ml cytochrome *c* to prevent adsorption of ω-Aga-IVA to reservoirs or tubing. External solutions were exchanged in less than a second by moving the cell between continuously flowing solutions from the perfusion tubes. Potentials reported are uncorrected for a liquid junction potential of −2 mV between the pipette solution and the Tyrode's solution in which the offset potential was zeroed before seal formation.

Synthetic ω-Aga-IVA was obtained from Peptides International (Louisville, KY) or as the kind gift of Dr. Nicholas Saccomano (Pfizer, Groton, CT). ω-Aga-IVA purified from the venom of *Agelenopsis aperta* was the kind gift of Dr. Michael Adams, University of California at Riverside. Both synthetic and purified ω-Aga-IVA powder were stored at −20°C for up to 4 years without loss of potency. Stocks were made as 100 μM in H_2O and stored at −20°C; in some cases, external recording solution was added directly to the powdered toxin.

To get better resolution of tail current kinetics, most experiments were done at 10–12°C, with the chamber cooled by circulating 3°C water through copper tubing that cooled a copper plate under the chamber. The temperature was measured using a thermistor in the bath. Experiments studying relief of inhibition by trains of depolarizations were carried out at room temperature (20–22°C), where both relief and reestablishment of inhibition were markedly more rapid. Action potential measurements were made at 35°C.

Statistics are given as mean ± standard error of the mean.

RESULTS

Voltage dependence

Fig. 1 shows the effect of 600 nM ω-Aga-IVA on P-type calcium channel current elicited from a cerebellar Purkinje neuron over a wide range of voltages. As described previously (Mintz et al., 1992a; Mintz and Bean, 1993), ω-Aga-IVA virtually eliminated inward current elicited by steps from −40 mV to ~+40 mV. Voltage steps positive to the reversal potential (about +60 mV) elicited outward currents, and these currents were affected much less by ω-Aga-IVA. This outward current is carried by internal Cs flowing outward through P-type calcium channels, because it is lacking if Cs is replaced by TEA or *N*-methyl-D-glucamine (Fig. 14), and is blocked by La (Fig. 1), Cd (Fig. 2), or ω-conotoxin MVIIC (not shown), another toxin that blocks P-type channels (Hillyard et al., 1992; McDonough et al., 1996). In the cell of Fig. 1, the outward current at +130 mV was reduced by only 15%. Although toxin had relatively little effect on the maximum current at +130 mV, the activation kinetics of the current were slowed; the control current was at maximum within 3 ms, but the current in ω-Aga-IVA continued to increase for at least 10 ms.

Apparently, block by ω-Aga-IVA is voltage-dependent, so that current is blocked almost completely for small depolarizations but not large depolarizations. Because the transition occurs at voltages near the reversal potential, where test pulse currents are small, the voltage dependence can be seen most clearly by analysis of tail currents following the test pulse. The tail current measured at −60 mV is plotted versus test pulse voltage in Fig. 1 *C*. In control, the activation curve could be described fairly well by a Boltzmann function, with a midpoint (V_h) of −3 mV and a slope factor (k) of 8 mV. In the presence of ω-Aga-IVA, the activation curve was shifted in the depolarizing direction, with a midpoint of +52 mV, and was more shallow, with a slope factor of 19 mV. The results in Fig. 1 were typical: in nine neurons studied with the same protocol, the midpoint shifted from −9 ± 2 mV in control to +44 ± 3 mV in ω-Aga-IVA, and the slope factor changed from 9 ± 1 mV to 19 ± 1 mV. In addition to the change in voltage dependence, the peak tail current elicited by the largest depolarizations was usually (but not always) smaller in ω-Aga-IVA than in control. In the same nine neurons, the reduction of peak tail currents by ω-Aga-IVA ranged from 0 to 45%, with an average reduction of 26% ± 5%. Cells with smaller tail currents in ω-Aga-IVA also displayed correspondingly smaller outward currents than in control at a given voltage (compare outward current at and tail current after the step to +130 mV in Fig. 1 *A*).

These results suggest that ω-Aga-IVA inhibits inward current through P-type calcium channels by modifying channel gating, so that channels no longer open significantly with moderate depolarizations. With toxin present, channels can be opened by large depolarizations, but with slower kinetics than in control. The slowed kinetics may represent slowed activation of channels that remain toxin-bound throughout, or it may simply represent the time for the toxin to dissociate from the channels, with subsequent opening of unbound channels. The cartoon in Fig. 2 illustrates these two possibilities. In the first case, OT channels would be conducting, with the CT-to-OT transition slower

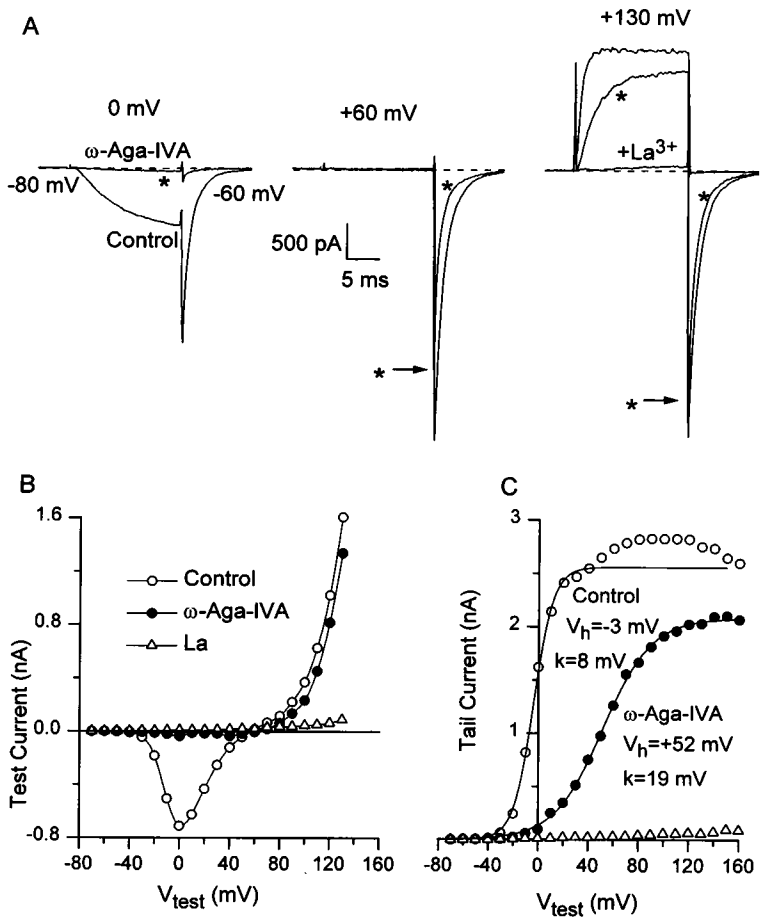

FIGURE 1 Inhibition by 600 nM ω-Aga-IVA of inward and outward calcium channel currents in a Purkinje neuron. (*A*) Current elicited by steps to 0 mV (*left*), +60 mV (*middle*), and +130 mV (*right*) in the absence and presence (*) of 600 nM ω-Aga-IVA. Outward currents and inward tail currents were blocked completely by 300 μM La. (*B*) Test pulse current (measured at end of 15-ms test pulse) versus test voltage in control (○), 600 nM ω-Aga-IVA (●), and 300 μM La (△). (*C*) Peak tail current versus test voltage. Solid lines are drawn according to the Boltzmann function, $I_{max}/(1 + \exp(-(V - V_h)/k))$, where I_{max} is the maximal tail current, V_h is the midpoint, and k is the slope factor. Fit to control points ignored points positive to +40 mV. The activation above the fit may be due to endogenous G protein modulation of the channels; the falling phase is due to large depolarizations that drive the channels into a second open state associated with lower current amplitudes (see Fig. 7). T = 10°C.

than the C-to-O transition. In the second case, OT channels would be nonconducting, and activation by large depolarizations would correspond to the OT-to-O transition.

The experiments in Fig. 3 and Fig. 4 tested whether the activation of channels at positive voltage is due to unbinding of toxin. In the presence of ω-Aga-IVA, current elicited by a step to 0 mV was still inhibited when the step was given 20 ms after a step to +150 mV, which activated substantial current (Fig. 3). Because block by 400 nM toxin occurs with a time constant of ~30 s at 10°C, it is very unlikely that toxin unbinds and then rebinds on the time scale of tens of milliseconds. The result in Fig. 3 therefore suggests that toxin remains bound to the channels during activation of current at +150 mV.

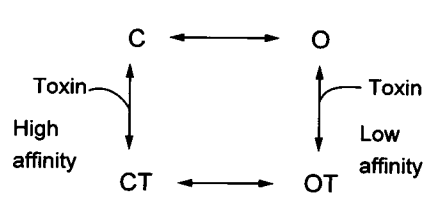

FIGURE 2 Model of ω-Aga-IVA interaction with the P-type calcium channel. Toxin (*T*) binds to closed (*C*) channels with high-affinity. Binding to open channels (*O*) is hypothesized to be much weaker. With strong depolarizations, toxin-bound channels (*CT*) may open (*OT*).

Fig. 4 shows another test of whether toxin remains bound when channels are opened by large depolarizations. A 30-ms step to +150 mV was followed by a 200-ms step to 0 mV. In control, there was little relaxation during the step to 0 mV, as expected, because control activation is nearly as complete at 0 mV as at +150 mV (e.g., Figs. 1 and 6). However, in the presence of toxin, the current at 0 mV decays considerably within 20 ms, so that steady-state current is only a fraction of the initial current at 0 mV. We interpret this relaxation as reflecting closing of toxin-bound channels that were opened by the step to +150 mV but are unable to remain open at 0 mV. If this interpretation is correct, the time course of decay at 0 mV reflects intrinsic kinetics of channels that remain toxin-bound throughout the protocol. If so, this relaxation should not be influenced by the toxin concentration, as long as it is sufficiently high that nearly all channels are bound. An alternative possibility is that toxin comes off the channels during the step to +150 mV and that the relaxation at 0 mV represents rebinding of toxin. In this case, the relaxation should be faster in higher toxin concentrations, because of the law of mass action. We tested these alternatives by performing the experiment in two concentrations of toxin, 50 nM and 400 nM, both of which produce saturating inhibition. The relaxations in the two concentrations superimposed, consistent with gating of

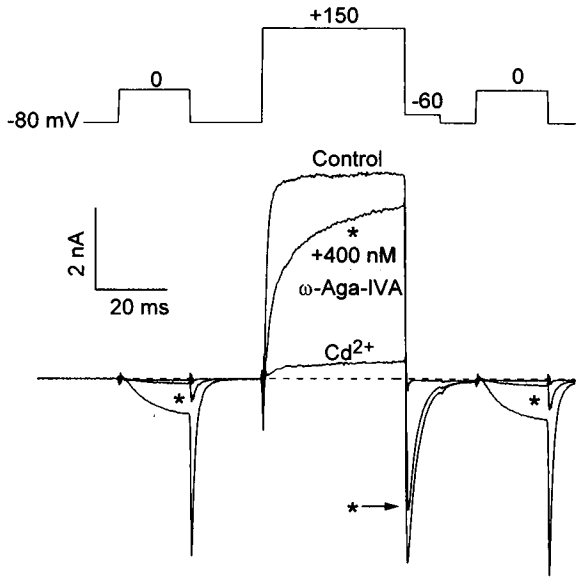

FIGURE 3 Persistence of ω-Aga-IVA binding after a large depolarization. Outward current was evoked by a 40-ms step to +150 mV, bracketed by 20-ms test pulses to 0 mV, before and after (*) inhibition by 400 nM ω-Aga-IVA. The protocol was repeated in 300 μM Cd, which blocked outward as well as inward current. T = 10°C.

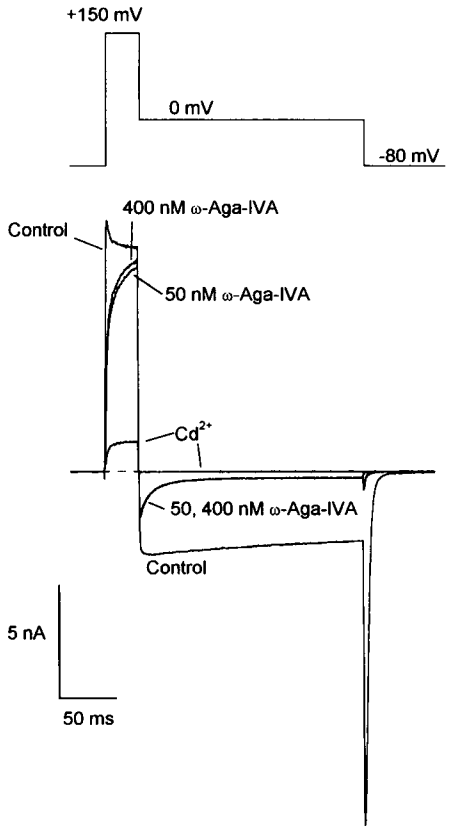

FIGURE 4 Relaxation of current at 0 mV after activation at +150 mV. With ω-Aga-IVA, the shift in voltage dependence causes a decaying tail current at 0 mV, whereas there is minimal decay in the control. The tail current at 0 mV superimposes for the two ω-Aga-IVA concentrations, suggesting that the relaxation is not due to rebinding of toxin. Channels were opened maximally by a 30-ms pulse to +150, then stepped to 0 mV for 200 ms. Initial block was with 400 nM purified ω-Aga-IVA, and then the cell was switched to 50 nM ω-Aga-IVA. The protocol was then repeated with Cd (300 μM). T = 10°C.

channels that remain toxin-bound throughout. Thus it seems likely that the slow activation of outward current at positive voltages and subsequent inward tail current reflect slowed opening of channels with toxin still bound.

At all voltages where significant current was activated in the presence of ω-Aga-IVA, the kinetics of current activation were strikingly slower in the presence of toxin (Fig. 5). Activation kinetics could be followed with best resolution by following the growth of tail currents after test pulses of increasing duration. An example is shown in Fig. 5 *A*. The envelope of tail currents after pulses to +90 mV could be fit well by a single exponential function with a time constant of 1.4 ms in control; in the presence of 400 nM ω-Aga-IVA, the maximum amplitude of the tail current was reduced, reflecting less than complete activation at +90 mV, and the time constant was 3.7 ms. Similar results were obtained at other voltages, with the differences in time constants and steady-state current amplitudes being most pronounced for smaller depolarizations (Fig. 5 *B* and *C*). With depolarizations large enough to evoke clear outward current, the slower development of tail currents was paralleled by slower development of outward currents. The time course of activation was the same when measured by development of outward current or by the envelope of tails (not shown).

The slower kinetics of activation in the presence of toxin raises the question of how much the changes in the activation curve, as measured in Fig. 1, may reflect changes in channel kinetics rather than a true change in the voltage dependence of activation. The 15-ms test pulses used to determine the activation curves may be too short to allow activation to reach equilibrium in the presence of toxin. The experiment in Fig. 6 tested the degree to which activation curves defined with a conventional protocol are affected by slowed kinetics of toxin-bound channels. Activation curves were determined with test pulses given either from −80 mV (where activation is zero) or after a 30-ms prepulse to +150 mV, sufficient to give maximum activation both with and without toxin. Without a prepulse, currents activated during the test pulse; with a prepulse, currents deactivated during the test pulse. In control, activation curves were little different with or without the prepulse (V_h = −20 mV), suggesting that equilibrium is nearly reached from both directions. With toxin, the activation curve was significantly different with the prepulse (with the midpoint ~30 mV more negative) than without, but still much more positive and more shallow than in control. Because the two curves in toxin in Fig. 6 (*filled symbols*) represent approaches to equilibrium from opposite directions, the true equilibrium activation values must lie somewhere between the two curves, with midpoints of +13 mV and +41 mV. Thus the shift in the midpoint of steady-state activation is at least +33 mV (+39 ± 3 mV in collected results from four experiments).

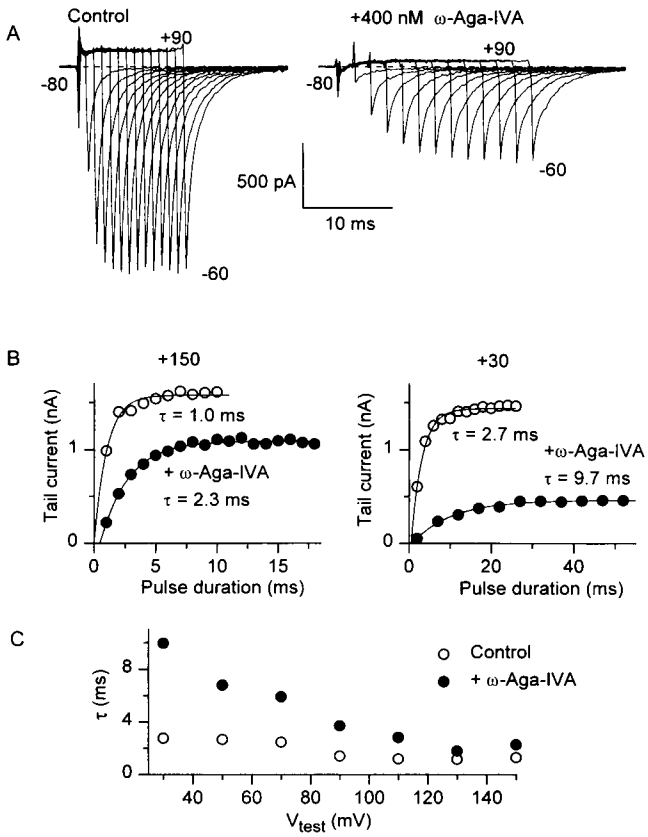

FIGURE 5 Slowing of channel activation by ω-Aga-IVA. (*A*) Tail currents at −60 mV measured in response to depolarizing voltage pulses to +90 mV. Currents were measured in controls and after complete inhibition by (and in the continual presence of) 400 nM ω-Aga-IVA. In controls, the voltage pulse was incremented at 1-ms intervals; in ω-Aga-IVA, the voltage pulse was incremented at 2-ms intervals. After each voltage pulse in ω-Aga-IVA, current at −10 mV was monitored to ensure that ω-Aga-IVA was not unbinding appreciably during the voltage pulse. Acquisition was paused for 4 s between successive voltage pulses to allow rebinding of any ω-Aga-IVA that had dissociated from the channel. (*B*) Exponential fits of channel activation in control and after block by ω-Aga-IVA, for V_{test} = +150 mV and +30 mV. Each point represents peak tail current from a pulse like those in *A*. (*C*) Time constants of current activation, in control and in ω-Aga-IVA, as a function of test voltage. T = 10°C.

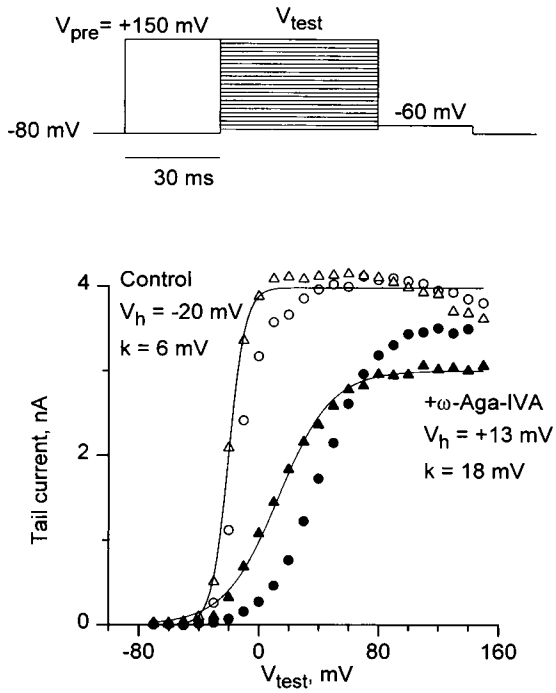

FIGURE 6 ω-Aga-IVA-induced shift in the voltage dependence of activation, with and without a fully activating prepulse. ○, △, control; ●, ▲, with 400 nM ω-Aga-IVA. ○, ●, Tail currents evoked by a 15-ms test pulse to the indicated voltage, as in Fig. 1. △, ▲, A 50-ms test pulse was preceded by a 30-ms pulse to +150 mV, as shown. The 30-ms prepulse is long enough to maximally activate channels both in control and with ω-Aga-IVA (see Fig. 5 *B*). Fits are single Boltzmann functions fitted to activation curves with the prepulse (△, ▲). Control, V_h = −20 mV, k = 6 mV; with ω-Aga-IVA, V_h = +13 mV, k = 18 mV. Curves without a prepulse (○, ●) were also fitted to single Boltzmann functions (fits not shown) with V_h = −12 mV, k = 8 mV (control) and V_h = +41 mV, k = 17 mV (ω-Aga-IVA). The decline of control tail currents at very strong depolarizations may reflect channel entry into an second open state with lower conductance (see Fig. 8). T = 10°C.

The shift in the voltage dependence of activation and the slowing of activation kinetics are both consistent with the general idea that binding of toxin stabilizes closed states of the channel. Fig. 7 shows that the tail currents after channel activation (by a pulse to +150 mV) are slightly faster in the presence of toxin (at −60 mV, time constant of 1.5 ms in control and 0.9 ms with toxin). This is consistent with the idea that the open state (or states) of the channel are destabilized when toxin is bound.

In examining the alteration of deactivation kinetics by toxin, we obtained results suggesting that P-type channels can occupy multiple open states. The kinetics of deactivation changed with the duration of the activating voltage pulse. With deactivation tail currents measured at −35 mV, deactivation began instantly after short pulses (<5 ms) to +50 mV, but had a distinct sigmoidicity after a 10-ms activating pulse (Fig. 8 *A*). The sigmoidicity was not due to slow voltage clamp, because the tail current elicited by a 4-ms activation pulse decayed with normal exponential kinetics, as did larger tail currents recorded at more negative voltages (not shown). One possible interpretation is that after the 10-ms pulse to +50, some channels are in a second open state from which they cannot close directly. The peak of the sigmoidal tail current had a slightly smaller amplitude than the peak of the exponential tail current, as if the second open state has a lower conductance than the initial open state. Fig. 8 *B* shows another voltage protocol that elicits currents consistent with this idea. A voltage step to +110 mV elicited outward current that reached a peak in ~2 ms and then decayed by about 25% over 10 ms. The decay of the outward current was correlated with changes in the kinetics of the tail currents on repolarization to −50 mV; with increasing time at +110 mV, the tail currents were initially sharp and exponential, but gradually decayed more slowly and developed an initial sigmoidal phase as pulse duration increased. The changes in tail current kinetics

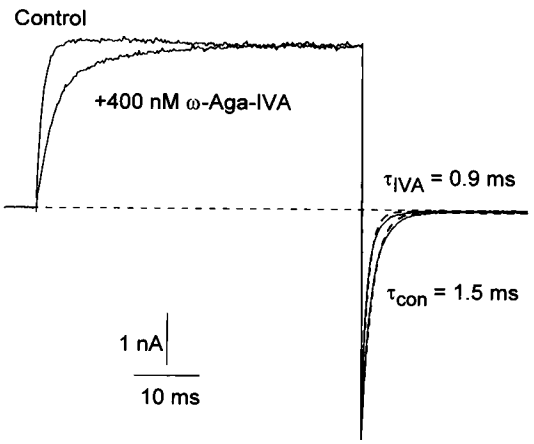

FIGURE 7 Faster deactivation with ω-Aga-IVA. Traces are from a 50-ms step to +150 mV, with tail current at −60 mV, before and after inhibition by 400 nM ω-Aga-IVA. Tail currents are fit by a single exponential decay function (– – –). T = 10°C.

seemed correlated with the decrease in amplitude of both outward current and initial tail current, which occurred in parallel. With tail currents at less negative voltages, there was a distinct rising phase rather than a simple sigmoidal decay (Fig. 8 *C*). These effects are consistent with occupancy of a second open state with lower conductance; an alternative possibility that cannot be excluded is that the apparent reduction of conductance reflects rapid equilibrium with a closed state.

Changes in tail current kinetics with the duration of the activating pulse were still present when channels were modified by ω-Aga-IVA. Fig. 9 shows current in response to pulses to +110 mV of increasing duration, followed by tail currents at −50 mV. Both outward current and inward tail current were at maximum for a 2-ms depolarization to +110 mV and decreased with longer depolarizations. Deactivation at −50 mV could be fit well by a single exponential, with a time constant that increased from 1.8 ms after a 1-ms depolarization to 4.4 ms after a 10-ms depolarization. After modification by ω-Aga-IVA, outward current at +110 mV activated more slowly, taking ~6 ms to reach maximum. Deactivation at −50 mV became slower with increasing length of depolarization, but for a given length of depolarization, it was about 50% faster than in control. If the changes in tail current kinetics reflect occupancy of two open states, these results suggest that both states can be occupied when channels are toxin-bound.

The results so far show that toxin-bound channels activate and deactivate with greatly altered kinetics. Are the permeation properties of the channel as well as its gating properties altered by bound toxin? We tested this by measuring the current-voltage relationship for fully activated channels with and without toxin (Fig. 10). There was no change in the reversal potential or the shape of the current-voltage relation, suggesting that permeation properties of toxin-bound channels, once they are opened by large depolarizations, are little different from control.

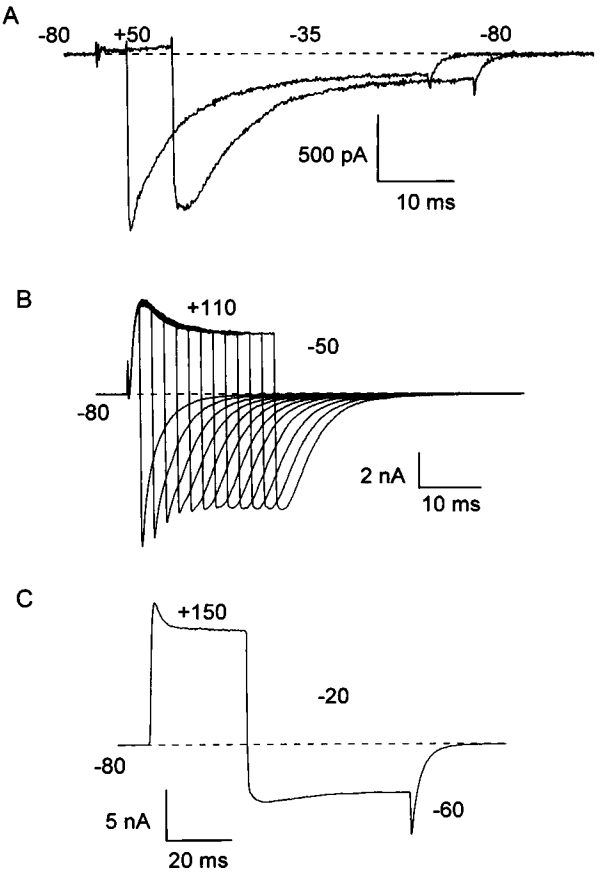

FIGURE 8 Changes in tail current kinetics with duration of the activating pulse. Data from three separate cells in the absence of toxin. The dashed line represents the zero current level. (*A*) Tail currents at −35 mV after a 4-ms and a 10-ms pulse to +50 mV. Tail current after the 4-ms step decays exponentially, whereas the decay after the 10-ms step is sigmoidal. (*B*) Voltage steps to +110 mV incremented at 2 ms, tail currents measured at −50 mV. Leak subtraction was performed by subtracting an identical protocol taken in 300 μM Cd. (*C*) Possible transition between open states reflected by relaxations at voltages of +150 mV and −20 mV. T = 10°C.

Because inhibition by ω-Aga-IVA involves dramatic changes in the voltage dependence of channel activation, we expected that the toxin might produce alterations in the gating current that must accompany the opening of the channels. We recorded nonlinear charge movement from Purkinje neurons with voltage steps directly to the Ca reversal potential, or at many voltages after blocking ionic current by replacing Ba with 2 mM Cd and 0.1 mM La. ω-Aga-IVA had no resolvable effect on the maximum charge movement or on its voltage dependence. The saturating charge movement averaged 90 ± 10 fC (n = 10). By nonstationary fluctuation analysis (Sigworth, 1980), the estimated number of P-type channels was 10,140 ± 2,410 (n = 8). This predicts ~20 fC of charge movement from P-type Ca channels, assuming movement of 9 e_0 per channel (Noceti et al., 1996). We might have expected to detect complete abolition of gating charge from P-type channels by ω-Aga-IVA, but any more subtle effect would likely have been too small for us to detect.

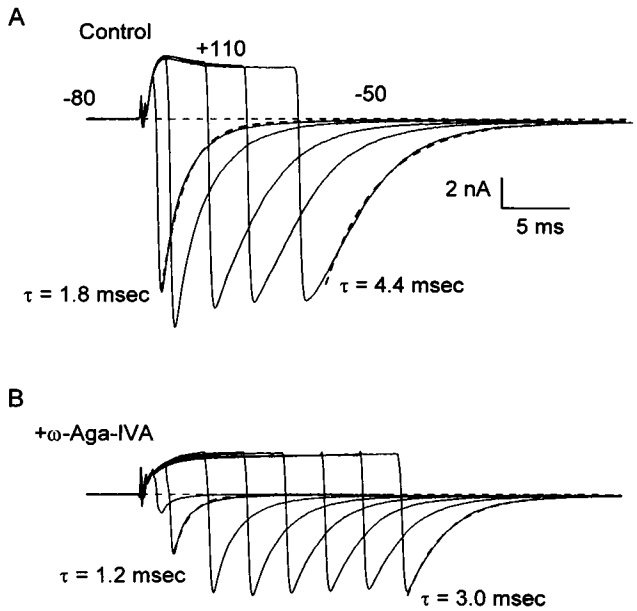

FIGURE 9 Effect of ω-Aga-IVA on tail current at −50 mV with different lengths of activation at +110 mV. Decay time constants are slower with increasing length of depolarization, both in control and in ω-Aga-IVA. The single exponential fit (– – –) is superimposed over the first and last tail currents in control and in ω-Aga-IVA, with time constants as shown. Note that the tail current for the longest pulse has a sigmoidal decay in control, but not in ω-Aga-IVA. T = 10°C.

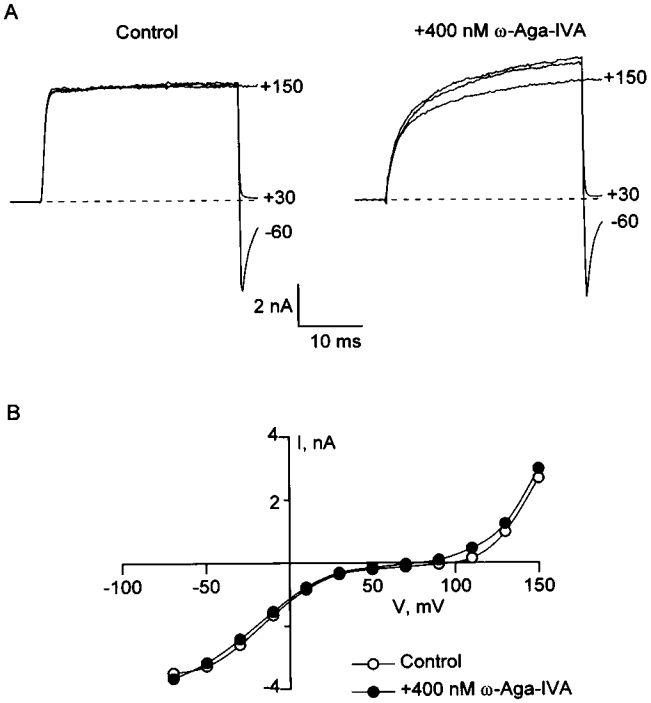

FIGURE 10 Lack of effect of ω-Aga-IVA on instantaneous current-voltage relationship. (*A*) Channels were opened fully with a 30-ms prepulse to +150, then instantaneous current was measured with a 3-ms step to the test voltage, before and after inhibition by 400 nM ω-Aga-IVA. Currents are leak-subtracted using scaled currents from a pulse to −90 mV. (*B*) Tail current versus voltage. Currents in *A* are plotted, with currents that remained in 300 μM Cd subtracted. T = 10°C.

P-type calcium channels in Purkinje neurons inactivate slowly with maintained depolarizations (Regan, 1991). Previous experiments showed that with two second prepulses (and 5 mM Ba as charge carrier), the midpoint of inactivation was about −40 mV, and for potentials at which there was significant inactivation, there was also some activation of channels (Regan, 1991). In a variety of other voltage-dependent channels, inactivation is coupled more or less tightly to channel opening. We tested whether the positive shift in activation gating by ω-Aga-IVA would result in a change in the voltage dependence of inactivation. Fig. 11 shows an experiment in which the voltage dependence of inactivation was determined with and without ω-Aga-IVA, using as test pulses depolarizations large enough to elicit current both in control and with toxin. In the presence of ω-Aga-IVA, the voltage dependence of inactivation was shifted in the depolarizing direction and had a shallower dependence on voltage. The midpoint of the inactivation curve determined with four second prepulses shifted from −27 ± 2 mV in control (n = 6) to −9 ± 1.5 mV in toxin (n = 7), and the slope factor changed from 7 ± 1 mV in control to 11 ± 1 mV in toxin.

Inhibition by ω-Aga-IVA can be relieved by a train of large depolarizing pulses (Mintz et al., 1992a). This relief of block is consistent with physical dissociation of the toxin molecule from the channel, because if toxin is still present in the external solution, block redevelops with the same kinetics as for the initial toxin application. Figs. 12 and 13 show how the relief of block by trains of depolarizing pulses depends on voltage and time. (Unlike the experiments described so far, this series of experiments was performed at room temperature, because relief was too slow at 10°C to be easily studied.) The experiment in Fig. 12 *A* examined the ability of trains of pulses to different voltages to relieve toxin block. Current was measured during 20-ms depolarizations to −20 mV, delivered every 6 s. At the times shown by arrows, a train of ten 50-ms depolarizing pulses was delivered. Such trains had no effect on control currents (*leftmost arrow*). After block by 400 nM ω-Aga-IVA, the depolarizing trains induced partial relief of block. The extent of relief depended on the voltage during the train, with 10 pulses to +70 mV producing about 20% relief, 10 pulses to +100 mV about 40%, and 10 pulses to +130 mV about 70% relief. Two trains of 10 pulses to +130 mV produced complete relief.

The time course of relief during the depolarizing trains was monitored by interspersing short (20 ms) test pulses to −20 mV with the large depolarizing pulses. Fig. 12 *B* shows the structure of the depolarizing trains; each 50-ms step to a positive voltage was followed by a 30-ms return to −70 mV and a 20-ms step to −20 mV, where test current was measured. As shown in Fig. 12 *C*, in control the currents at −20 mV (*circled*) were unaffected by the step to +130 mV; test currents maintained a constant amplitude of 2 nA. After

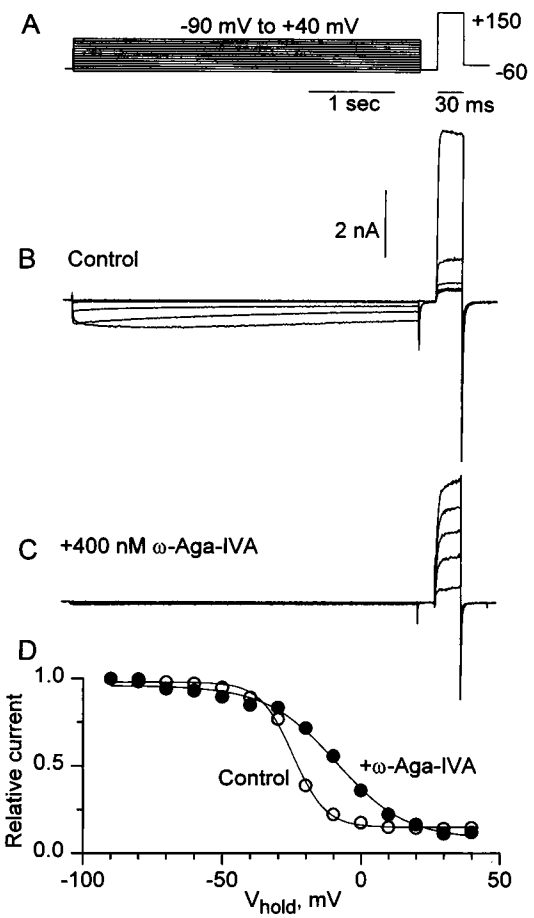

FIGURE 11 Alteration of voltage dependence of inactivation by 400 nM ω-Aga-IVA. (*A*) Cell was held for 4 s at holding potentials from −90 mV to +40 mV. After a brief (20 ms) return to −80 mV to allow deactivation of current, inactivation was assayed by a 30-ms pulse to +150 mV, followed by tail current at −60 mV. Traces shown are with holding potentials of −50, −20, −10, 0, and +20 mV, in control (*B*) and after inhibition by 400 nM ω-Aga-IVA. (*C*) Prepulse (holding) current is shown at compressed time base (note the 10-fold difference in horizontal scale bars). (*D*) Tail current as a function of holding potential, normalized to the peak current in control (○) and in toxin (●). T = 10°C.

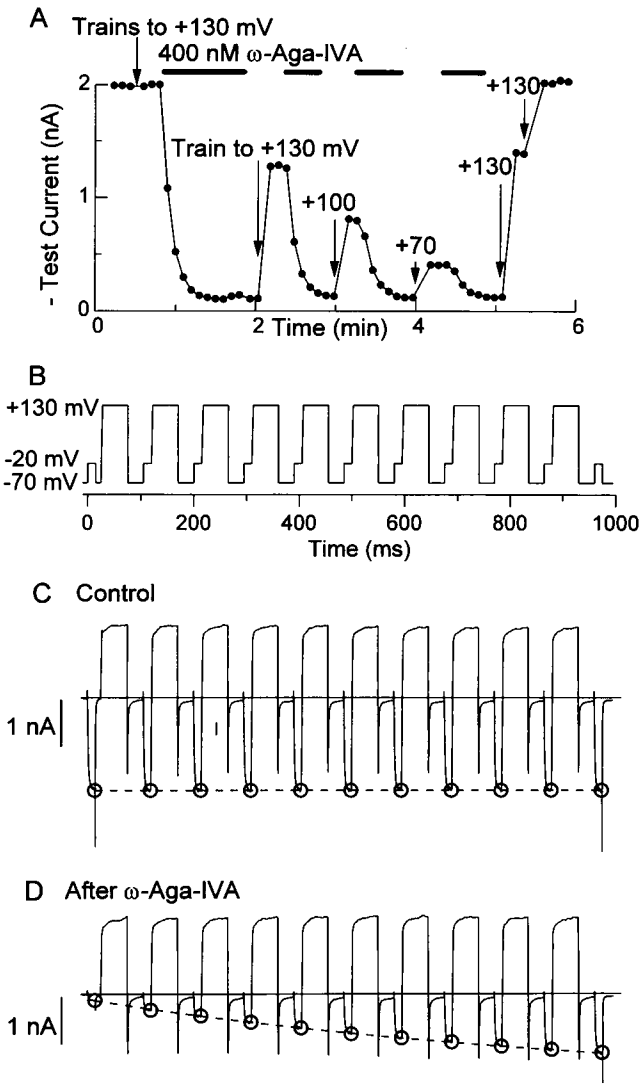

FIGURE 12 Removal of ω-Aga-IVA inhibition by trains of large depolarizations. (*A*) Current at −20 mV during block, knockoff, and reblock by 400 nM ω-Aga-IVA. (*B*) Voltage protocol for the depolarizing trains. The cell was given ten 50-ms pulses to the indicated voltage, while current was monitored at −20 mV after each pulse. (*C*) Depolarizing trains had no effect on peak current at −20 mV (*circled*). (*D*) After ω-Aga-IVA, each successive large depolarizing pulse results in greater current at −20 mV. External solution: 160 mM TEACl, 5 mM $BaCl_2$, 10 mM HEPES, 1 mg/ml cytochrome *c*, pH adjusted to 7.4 with TEAOH. Internal (pipette) solution: 108 mM Cs-methanesulfonate, 4 mM $MgCl_2$, 9 mM EGTA, 9 mM HEPES, 4 mM MgATP, 14 mM creatine phosphate (Tris salt), 0.3 mM Tris-GTP, pH adjusted to 7.4 with CsOH. T = 22°C.

inhibition by ω-Aga-IVA, the test currents at −20 mV grew progressively larger after each pulse to +130 mV.

The relief of block could be fit well by a single exponential recovery function (Figs. 12 *D* and 13 *A*). The rate of recovery increased with increasing depolarization (Fig. 13 *B*). The rate constant increased steeply in the range from +50 mV to +120 mV and less steeply from +120 mV to +180 mV, the most positive potentials for which the pulse train did not damage the cell. The voltage dependence of the rate constant of recovery could be described fairly well by a Boltzmann function with a midpoint of +121 mV and a slope factor of 26 mV (Fig. 13 *B*).

Voltages of at least +50 mV were required to see significant relief. Because this corresponds roughly to the reversal potential of the channel with the internal Cs solutions used in most experiments, outward Cs current flowed at the voltages at which inhibition was relieved. One possibility is that the relief results from knock-off of the toxin by permeating Cs ions, similar to relief of charybdotoxin inhibition of potassium channels by outwardly permeating K ions (MacKinnon and Miller, 1988). To test this possibility, the relief protocols were performed with TEA or *N*-methyl-D-glucamine (NMDG) as the main internal cation. Neither of these carries outward current through the channel (see Fig. 14 *A*). Nevertheless, trains of depolarizations still relieved ω-Aga-IVA inhibition, and the rate constant of relief as a

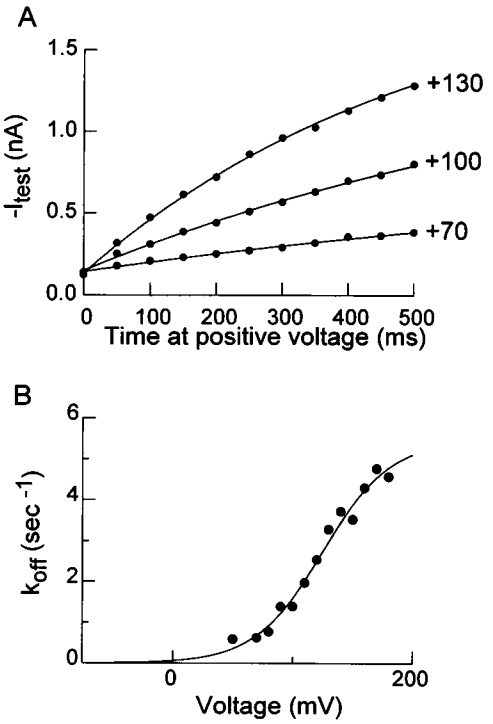

FIGURE 13 Voltage dependence of removal of ω-Aga-IVA inhibition. Data are collated from the cell in Fig. 12. (*A*) Current at −20 mV as a function of total time spent at the indicated voltage. (*B*) Recovery rate (from exponential fits as in *A*) as a function of voltage. T = 22°C.

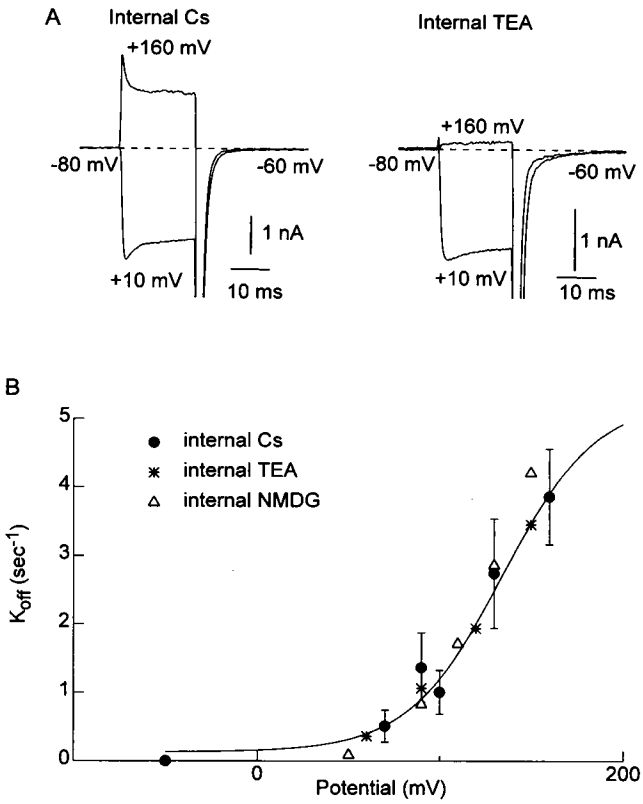

FIGURE 14 Depolarization-induced relief of ω-Aga-IVA inhibition with permeant and impermeant internal cations. (*A*) Current at +10 mV and +160 mV with Cs (*left*) and TEA (*right*) as the main cation in the internal (pipette) solution. Solutions otherwise as in Fig. 12. (*B*) Recovery rate as a function of voltage with different internal cations. Each point with Cs is an average of off-rates from four to six cells. T = 22°C.

function of voltage was not significantly different from the experiments using internal Cs (Fig. 14 *B*).

DISCUSSION

These experiments suggest that ω-Aga-IVA inhibits inward current through calcium channels by affecting the gating machinery of the channel, not by occluding the pore. The shift in the midpoint of channel activation is so large (~+50 mV) that there is almost no opening of channels at voltages where there is substantial driving force for Ca influx. If subjected to large enough depolarizations, however, channels can still open with toxin bound and appear to have permeation properties identical to control.

Many other toxins that target voltage-gated ion channels appear to act by blocking the channel pore. Examples include tetrodotoxin block of sodium channels (Hille, 1992), charybdotoxin block of maxi K channels, and agitoxin block of *Shaker* family K channels (see Miller, 1995, for review). Of calcium channel-blocking peptides, only the N-type channel blocker ω-conotoxin GVIA has been studied mechanistically. ω-CgTx-GVIA blocks current equally well at all voltages, including for very positive depolarizations, consistent with a pore-blocking mechanism (Boland et al., 1994), and the toxin appears to interact with glutamate residues forming the selectivity filter on the outer mouth of the pore (Ellinor et al., 1994).

Several potassium channel toxins alter channel gating in a manner that may be analogous to the effects of ω-Aga-IVA. The scorpion toxin noxiustoxin (α-KTx-2.1) blocks axonal K channels with lower potency at depolarized potentials, and the block is relieved by repetitive depolarizations in a K-independent manner (Carbone et al., 1987). Hanatoxin, from tarantula venom, inhibits cloned Kv2.1 channels in a voltage-dependent manner, with more inhibition for smaller depolarizations. Interestingly, the toxin appears not to interact with the pore region of the channel (Swartz and MacKinnon, 1995).

Block of calcium entry during action potentials

To interpret experiments that use ω-Aga-IVA to investigate the physiological role of P-type calcium channels, it is important to determine whether action potentials give significant activation of ω-Aga-IVA-bound channels. Modulation of calcium channels by neurotransmitters can be quantitatively different, depending on whether the currents are evoked by an action potential or step depolarizations (e.g., Penington et al., 1992; Pfrieger et al., 1994; Wheeler et al., 1996; Toth and Miller, 1995). In principle, there could be Ca influx through toxin-bound channels, because action

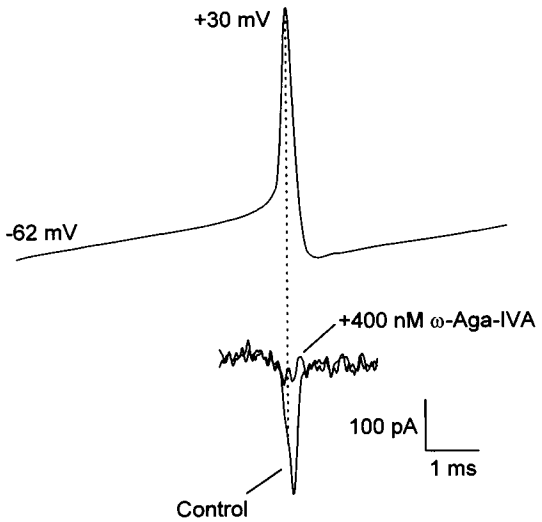

FIGURE 15 Effect of ω-Aga-IVA on calcium entry through P-type channels evoked by an action potential waveform. (*A*) Spontaneous action potential recorded from a Purkinje cell using an Axoclamp-2A amplifier (Axon Instruments). Corner filter frequency, 10 kHz, sampled at 20 μs. External solution: Tyrode's as in Materials and Methods. Internal solution: 122 mM KCl, 9 mM HEPES, 9 mM EGTA, 1.8 mM $MgCl_2$, 4 mM MgATP, 14 mM creatine phosphate (Tris salt), 0.3 mM GTP (Tris salt), pH 7.4, with KOH to total $[K^+]$ = 142 mM. Action potential recorded at 35°C. (*B*) Currents recorded from a Purkinje cell voltage-clamped with the action potential waveform in *A*, in control and in 400 nM ω-Aga-IVA. Dotted line indicates time at which the action potential is at its maximum overshoot. External solution: 160 mM TEA-Cl, 10 mM HEPES, 2 mM $CaCl_2$, 2 mM $MgCl_2$, 1 mg/ml cytochrome C, 1 μM tetrodotoxin, 5 μM nimodipine, 1 μM ω-CgTx-GVIA. Cell was held at −50 mV to inactivate T-type calcium channels fully. To eliminate current from capacitative artifacts, the current recorded was summed with the current evoked by five hyperpolarizing commands, each one-fifth the amplitude of the action potential. Current in 300 μM Cd was subtracted from current recorded in control and in ω-Aga-IVA. For the cell shown, the pipette resistance was 1.5 MΩ, and the product of uncompensated series resistance and membrane capacitance was ~8 μs. T = 35°C.

potentials can reach peak voltages of ~ +30 mV, where the fractional activation from rest of ω-Aga-IVA-bound channels is ~25% maximal (Fig. 1). To test this directly, spontaneous action potentials were recorded at 35°C from Purkinje neurons in Tyrode's solution under current clamp conditions. The action potential waveform was then used as the command stimulus in a voltage-clamp experiment (also at 35°C). Current was carried by a physiological concentration of calcium (2 mM), and P-type calcium channel currents were isolated by including TEA, tetrodotoxin, nimodipine, and ω-CgTx-GVIA in the external solution. The cell shown was held at −50 mV to inactivate T-type channels and remove the large component of the action potential-driven calcium current due to entry through T-type channels (see McCobb and Beam, 1991). Maximum calcium current occurred during the repolarization phase of the action potential (cf. Llinás et al., 1982; Wheeler et al., 1996), although there was some calcium entry during the rising phase (Sabatini and Regehr, 1996). The Ca channel current evoked by the action potential was blocked completely by 400 nM ω-Aga-IVA. In four out of four cells studied with this protocol, ω-Aga-IVA blocked all Ca influx. Although it is likely that there would be some steady-state activation of ω-Aga-IVA-bound channels at the peak voltage of the action potential, evidently activation of toxin-bound channels is too slow to be appreciable during the action potential. The experiment shows that ω-Aga-IVA can be used to produce complete block of current through P-type channels during an action potential stimulus. This is consistent with experiments showing complete inhibition of synaptic transmission at some central synapses when ω-Aga-IVA is applied with the N-type channel blocker ω-conotoxin-GVIA (Takahashi and Momiyama, 1993; Wu and Saggau, 1994; Regehr and Mintz, 1994). It is also consistent with imaging experiments in which Ca entry in Purkinje cell axons in cerebellar slices was abolished completely by the addition of ω-Aga-IVA (Callewaert et al., 1996).

Strength of binding to closed and open states

The simple scheme in Fig. 2 can account for the main features of the interaction of ω-Aga-IVA with P-type calcium channels, assuming that toxin binds with very different affinity to closed and open states of the channel. Toxin binds tightly to the closed state of the channel. From previous experiments, the K_D for binding to closed channels is about 2 nM (Mintz et al., 1992b). With toxin bound, the closed state is stabilized and channels require much larger depolarizations to be activated. When opened by sufficiently large depolarizations, channels have a much decreased affinity for toxin. With prolonged occupancy of the open state, toxin unbinds, even if toxin is still present at 200–400 nM in the external solution. To account for nearly full recovery in the presence of these concentrations of toxin, the K_D for binding to open channels must be at least as high as 2 μM. The difference between binding to closed and open channels can be accounted for mainly by a greatly increased off rate for open channels, about 10,000 times faster than that for closed channels (Mintz et al., 1992a). Relief of ω-Aga-IVA action by repetitive depolarizations has been reported for channels in other cell types, including sensory, spinal cord, and hippocampal neurons (Mintz et al., 1992a); cerebellar granule neurons (Randall and Tsien, 1995; Tottene et al., 1996); and squid giant fiber lobe neurons (McFarlane and Gilly, 1996). This suggests that inhibition by an allosteric mechanism may be a common mechanism for inhibition by ω-Aga-IVA of different channel types.

The simple model in Fig. 2 ignores the existence of multiple closed states of the channel and, perhaps, multiple open states as well. A number of details of ω-Aga-IVA inhibition are not captured by the simple model. In the model, the rate of relief of inhibition by prolonged depolarization would be expected to match reasonably well with the degree of activation of toxin-bound channels. Instead, the rate constant for relief has a midpoint (+120 mV)

substantially more positive than the midpoint of the activation curve for toxin-bound channels (+50 mV). The difference might be related to the apparent existence of multiple open states of the channel; one possibility is that dissociation of toxin is much faster from the open state reached via stronger depolarizations. Multiple open states might also help account for the decrease in magnitude of maximum tail current usually seen with toxin, because the open state requiring longer or larger depolarizations may have a lower conductance (Fig. 8). The existence of multiple conductances of P-type channels has previously been suggested from single-channel recordings (Usowicz et al., 1992). Control channels activate quickly, and maximum tail current may reflect occupancy of the first, higher conductance, open state. With toxin, activation is slowed, and equilibrium between the two open states may occur as fast as channels can open, so that there is never preferential activation of the higher conductance state.

In a detailed study of the deactivation kinetics of ω-Aga-IVA-sensitive calcium channels of squid giant fiber lobe neurons, McFarlane (1997) found slower tail currents with increasing depolarization lengths, modeled as two open states separated by a closed state. In the squid channels, depolarizing pulses removed ω-Aga-IVA inhibition with the same time course as channels appeared to enter the second open state, suggesting that the faster off-rate of ω-Aga-IVA at more depolarized voltages resulted from lower toxin affinity for the second open state. Although there are major quantitative differences between Purkinje channels and giant fiber lobe channels in both gating kinetics and sensitivity to ω-Aga-IVA (which inhibits more weakly and unbinds much faster for the squid channels), it is striking that both of these ω-Aga-IVA-sensitive channels appear to have multiple open states connected by voltage-dependent transitions. We have no direct test of the possibility that toxin may unbind more rapidly from a second open state reached by larger or longer depolarizations, but this would be consistent both with McFarlane's result and with the 70-mV difference between half-maximal activation of channels and the voltage dependence of relief of inhibition.

The simple model in Fig. 2 does not account for the less steep activation curve in the presence of toxin compared to control. With a conventional protocol for measuring a tail current activation curve, the decreased steepness could reflect failure to reach steady-state activation with smaller depolarizations. However, this cannot be the only explanation, because the activation curve for toxin-bound channels is still less steep when steady state is approached from the opposite direction (Fig. 6). One simple hypothesis is that toxin may act by altering the gating of only one of the four S4 regions of the channel. In this hypothesis, three of the pseudo-subunits of the channel would gate with more or less normal voltage dependence, whereas the movement of the fourth subunit would be retarded by ω-Aga-IVA. The ability of the channel to reach an open state would be determined by the position of the fourth subunit. It would be expected that the voltage dependence of any single subunit would be less steep than that for opening of the channel as a whole (assuming that channel opening requires movement of gating charge from all four subunits over similar voltage ranges). Such a picture also predicts that toxin binding would alter gating current only slightly, much less than the alteration of ionic current.

Comparison with modulation by G proteins

The modulation of gating of P-type calcium channels by ω-Aga-IVA is similar to the voltage-dependent modulation of calcium channels by G proteins, as inferred from changes in voltage dependence and kinetics after activation of some G protein-coupled receptors (Marchetti et al., 1986; Bean, 1989; Elmslie et al., 1990) or direct introduction of intracellular βγ subunits of G proteins (Ikeda, 1996; Herlitze et al., 1996). As with external ω-Aga-IVA, internal G proteins can inhibit channels by a shift of the activation curve in the depolarizing direction (+75 mV, Bean, 1989; ~ +30 mV, Ikeda, 1991; +27 mV, Boland and Bean, 1993). Just as for ω-Aga-IVA inhibition, when G protein-modulated channels are activated by sufficiently large depolarizations, the kinetics of activation are much slower than in control, and deactivation is slightly faster (Boland and Bean, 1993; Elmslie et al., 1990). However, the off rate of G proteins during large facilitating pulses and the G protein on-rate after facilitation are 100- to 1000-fold faster than the corresponding rates for ω-Aga-IVA. In addition, the instantaneous current-voltage relationship for G protein-modulated N-type channels was found to be different from that of control (Kuo and Bean, 1993; but see Carabelli et al., 1996; Patil et al., 1996), whereas we saw no difference for ω-Aga-IVA-bound channels. The similarity of ω-Aga-IVA inhibition to G-protein inhibition does not imply any direct interaction between toxin and G-protein-binding sites, which are almost certainly on opposite sides of the membrane. Rather, it merely implies that both inhibit the channel by an allosteric mechanism involving stabilization of closed states.

Supported by the National Institutes of Health (HL35034).

REFERENCES

Adams, M. E., I. M. Mintz, M. D. Reily, V. Thanabal, and B. P. Bean. 1993. Structure and properties of ω-agatoxin IVB, a new antagonist of P-type calcium channels. *Mol. Pharmacol.* 44:681–688.

Bargas, J., A. Howe, J. Eberwine, U. Cao, and D. J. Surmeier. 1994. Cellular and molecular characterization of Ca^{2+} currents in acutely isolated, adult rat neostriatal neurons. *J. Neurosci.* 14:6667–6686.

Bean, B. P. 1989. Neurotransmitter inhibition of neuronal calcium currents by changes in channel voltage dependence. *Nature.* 340:153–156.

Boland, L. M., and B. P. Bean. 1993. Modulation of N-type calcium channels in bullfrog sympathetic neurons by luteinizing hormone-releasing hormone: kinetics and voltage dependence. *J. Neurosci.* 13: 516–533.

Boland, L. M., J. M. Morrill, and B. P. Bean. 1994. ω-Conotoxin block of N-type calcium channels in frog and rat sympathetic neurons. *J. Neurosci.* 8:5011–5027.

Callewaert, G., J. Eilers, and A. Konnerth. 1996. Axonal calcium entry during fast "sodium" action potentials in rat cerebellar Purkinje neurons. *J. Physiol. (Lond.).* 495:641–647.

Carabelli, V., M. Lovallo, V. Magnelli, H. Zucker, and E. Carbone. 1996. Voltage-dependent modulation of single N-type Ca^{2+} channel kinetics by receptor agonists in IMR32 cells. *Biophys. J.* 70:2144–2154.

Carbone, E., G. Prestipino, L. Spadavecchia, F. Franciolini, and L. D. Possani. 1987. Blocking of the squid axon K^+ channel by noxiustoxin: a toxin from the venom of the scorpion *Centruroides noxius*. *Pflügers Arch.* 408:423–431.

Eliot, L. E., and D. Johnston. 1994. Multiple components of calcium current in acutely dissociated dentate gyrus granule neurons. *J. Neurophysiol.* 72:762–777.

Ellinor, P. T., J.-F. Zhang, W. A. Horne, and R. W. Tsien. 1994. Structural determinants of the blockade of N-type calcium channels by a peptide neurotoxin. *Nature.* 372:272–275.

Elmslie, K. S., W. Zhou, and S. W. Jones. 1990. LHRH and GTP-γ-S modify calcium current activation in bullfrog sympathetic neurons. *Neuron.* 5:75–80.

Hamill, O. P., A. Marty, E. Neher, B. Sakmann, and F. J. Sigworth. 1981. Improved patch-clamp techniques for high-resolution current recording from cells and cell-free membrane patches. *Pflügers Arch.* 391:85–100.

Herlitze, S., D. E. Garcia, K. Mackie, B. Hille, T. Scheuer, and W. A. Catterall. 1996. Modulation of Ca^{2+} channels by G-protein βγ subunits. *Nature.* 380:258–262.

Hille, B. 1992. Ionic Channels of Excitable Membranes. Sinauer Associates, Sunderland, MA.

Hillyard, D. R., V. D. Monje, I. M. Mintz, B. P. Bean, L. Nadasdi, J. Ramachandran, G. Miljanich, Z. Azimi-Zoonooz, J. M. McIntosh, L. J. Cruz, J. S. Imperial, and B. M. Olivera. 1992. A new conus peptide ligand for mammalian presynaptic Ca^{2+} channels. *Neuron.* 9:69–77.

Ikeda, S. R. 1991. Double-pulse calcium channel current facilitation in adult rat sympathetic neurons. *J. Physiol. (Lond.).* 439:181–214.

Ikeda, S. R. 1996. Voltage-dependent modulation of N-type calcium channels by G-protein βγ subunits. *Nature.* 380:255–258.

Kuo, C.-C., and B. P. Bean. 1993. G-protein modulation of ion permeation through N-type calcium channels. *Nature.* 365:258–262.

Llinás, R., M. Sugimori, J.-W. Lin, and B. Cherksey. 1989. Blocking and isolation of a calcium channel from neurons in mammals and cephalopods utilizing a toxin fraction (FTX) from funnel-web spider poison. *Proc. Natl. Acad. Sci. USA.* 86:1689–1693.

Llinás, R., M. Sugimori, and S. M. Simon. 1982. Transmission by presynaptic spike-like depolarization in the squid giant synapse. *Proc. Natl. Acad. Sci. USA.* 79:2415–2419.

MacKinnon, R., and C. Miller. 1988. Mechanisms of charybdotoxin block of Ca^{2+}-activated K^+ channels. *J. Gen. Physiol.* 91:335–349.

Magnelli, V., A. Pollo, E. Sher, and E. Carbone. 1995. Block of non-L-, non-N-type Ca^{2+} channels in rat insulinoma RINm5F cells by ω-agatoxin IVA and ω-conotoxin MVIIC. *Pflügers Arch.* 429:762–771.

Marchetti, C., E. Carbone, and H. D. Lux. 1986. Effects of dopamine and noradrenaline on Ca^{2+} channels of cultured sensory and sympathetic neurons of chick. *Pflügers Arch.* 406:104–111.

McCobb, D. P., and K. G. Beam. 1991. Action potential waveform voltage-clamp commands reveal striking differences in calcium entry via low and high voltage-activated calcium channels. *Neuron.* 7:119–127.

McDonough, S. I., K. J. Swartz, I. M. Mintz, L. M. Boland, and B. P. Bean. 1996. Inhibition of calcium channels in rat central and peripheral neurons by ω-conotoxin MVIIC. *J. Neurosci.* 16:2612–2623.

McFarlane, M. B. 1997. Depolarization-induced slowing of Ca channel deactivation in squid neurons. *Biophys. J.* 72:1607–1621.

McFarlane, M. B., and W. F. Gilly. 1996. Spatial localization of calcium channels in giant fiber lobe neurons of the squid (*Loligo opalescens*). *Proc. Natl. Acad. Sci. USA.* 93:5067–5071.

Miller, C. 1995. The charybdotoxin family of K^+ channel-blocking peptides. *Neuron.* 15:5–10.

Mintz, I. M., M. E. Adams, and B. P. Bean. 1992a. P-type calcium channels in rat central and peripheral neurons. *Neuron.* 9:1–20.

Mintz, I. M., and B. P. Bean. 1993. Block of calcium channels in rat neurons by synthetic ω-Aga-IVA. *Neuropharmacology.* 32:1161–1169.

Mintz, I. M., V. J. Venema, K. Swiderek, T. Lee, B. P. Bean, and M. E. Adams. 1992b. P-type calcium channels blocked by the spider toxin ω-Aga-IVA. *Nature.* 355:827–829.

Noceti, F., P. Baldelli, X. Wei, N. Qin, L. Toro, L. Birnbaumer, and E. Stefani. 1996. Effective gating charges per channel in voltage-dependent K^+ and Ca^{2+} channels. *J. Gen. Physiol.* 108:143–155.

Patil, P. G., M. de Leon, R. R. Reed, S. Dubel, T. P. Snutch, and D. T. Yue. 1996. Elementary events underlying voltage-dependent G-protein inhibition of N-type calcium channels. *Biophys. J.* 71:2509–2521.

Penington, N. J., J. S. Kelly, and A. P. Fox. 1992. Action potential waveforms reveal simultaneous changes in I_{Ca} and I_K produced by 5-HT in rat dorsal raphe neurones. *Proc. R. Soc. Lond. (Biol.).* 248:171–179.

Pfrieger, F. W., K. Gottmann, and H. D. Lux. 1994. Kinetics of $GABA_B$ receptor-mediated inhibition of calcium currents and excitatory synaptic transmission in hippocampal neurons in vitro. *Neuron.* 12:97–107.

Randall, A., and R. W. Tsien. 1995. Pharmacological dissection of multiple types of Ca^{2+} channel currents in rat cerebellar granule neurons. *J. Neurosci.* 15:2995–3012.

Regan, L. J. 1991. Voltage-dependent calcium currents in Purkinje cells from rat cerebellar vermis. *J. Neurosci.* 11:2259–2269.

Regehr, W. G., and I. M. Mintz. 1994. Participation of multiple calcium channel types in transmission at single climbing fiber to Purkinje cell synapses. *Neuron.* 12:605–613.

Sabatini, B. L., and W. G. Regehr. 1996. Timing of neurotransmission at fast synapses in the mammalian brain. *Nature.* 384:170–172.

Sigworth, F. J. 1980. The variance of sodium current fluctuations at the node of Ranvier. *J. Physiol. (Lond.).* 307:97–129.

Swartz, K. J., and R. MacKinnon. 1995. An inhibitor of the Kv2.1 potassium channel isolated from the venom of a Chilean tarantula. *Neuron.* 15:941–949.

Takahashi, T., and A. Momiyama. 1993. Different types of calcium channels mediate central synaptic transmission. *Nature.* 366:156–158.

Toth, P. T., and R. J. Miller, 1995. Calcium and sodium currents evoked by action potential waveforms in rat sympathetic neurones. *J. Physiol. (Lond.).* 485.1:43–57.

Tottene, A., A. Moretti, and D. Pietrobon 1996. Functional diversity of P-type and R-type calcium channels in rat cerebellar neurons. *J. Neurosci.* 16:6353–6363.

Turner, T. J., M. E. Adams, and K. Dunlap. 1992. Calcium channels coupled to glutamate release identified by ω-Aga-IVA. *Science.* 258: 310–313.

Usowicz, M. M., M. Sugimori, B. Cherksey, and R. Llinás. 1992. P-type calcium channels in the somata and dendrites of adult cerebellar Purkinje cells. *Neuron.* 9:1185–1199.

Wheeler, D. B., A. Randall, and R. W. Tsien. 1994. Roles of N-type and Q-type Ca^{2+} channels in supporting hippocampal synaptic transmission. *Science.* 264:107–111.

Wheeler, D. B., A. Randall, and R. W. Tsien. 1996. Changes in action potential duration alter reliance of excitatory synaptic transmission on multiple types of Ca^{2+} channels in rat hippocampus. *J. Neurosci.* 16: 2226–2237.

Wu, L.-G., and P. Saggau. 1994. Pharmacological identification of two types of presynaptic voltage-dependent calcium channels at CA3-CA1 synapses of the hippocampus. *J. Neurosci.* 14:5613–5622.